

# Hybrid Invariance and Stability of a Feedback Linearizing Controller for Powered Prostheses

Anne E. Martin<sup>1</sup> and Robert D. Gregg<sup>2</sup>

**Abstract**—The development of powered lower-limb prostheses has the potential to significantly improve amputees’ quality of life. By applying advanced control schemes, such as hybrid zero dynamics (HZD), to prostheses, more intelligent prostheses could be designed. Originally developed to control bipedal robots, HZD-based control specifies the motion of the actuated degrees of freedom using output functions to be zeroed, and the required torques are calculated using feedback linearization. Previous work showed that an HZD-like prosthesis controller can successfully control the stance period of gait. This paper shows that an HZD-based prosthesis controller can be used for the entire gait cycle and that feedback linearization can be performed using only information measured with on-board sensors. An analytic metric for orbital stability of a two-step periodic gait is developed. The results are illustrated in simulation.

## I. INTRODUCTION

Currently, prostheses do not completely restore healthy human walking, partly due to the fact that most commercially available prostheses cannot produce positive work. In contrast, human joints generate significant positive work during gait [1]. To improve amputee gait quality, powered prostheses have been developed [2], [3]. The controllers typically divide the stride into five periods with a set impedance (stiffness, damping, and equilibrium point) for each period [2], resulting in large numbers of parameters to be tuned [4]. An alternative control approach is to vary the joint positions in a continuous manner, which may result in superior disturbance rejection and relieve the amputee of some of the cognitive and physical effort of gait. This strategy requires that the progression of the gait be parameterized in a unified manner, possibly by using a phase variable [5]–[7]. A phase variable is a kinematic quantity that measures how far a step has progressed. An additional advantage of the phase-based control approach is that it automatically adjusts for speed because the faster the amputee walks, the faster the phase variable increases.

A promising phase-based control framework is hybrid zero dynamics (HZD) from the field of bipedal robots. HZD-based control has successfully generated stable walking for both point [8] and curved [9] foot bipedal robots. In addition, it

has been used to predict healthy human walking [10]. Under an HZD-based control paradigm, bipeds are assumed to be underactuated, the step is driven by the progression of the phase variable, and each step is divided into a finite-time single support period and an instantaneous impact during which the stance leg switches [8]. During the single support period, the motion of the actuated degrees of freedom (DoF) are encoded in output functions to be zeroed. The required joint torques are determined using feedback linearization. The motion of the unactuated DoF are captured in the zero dynamics. Since gait is typically assumed to be one-step periodic, orbital stability can be evaluated using the method of Poincaré. If the desired gait respects the impact dynamics (i.e. is hybrid invariant), then orbital stability can be evaluated using just the lower-dimensional zero dynamics.

One of the challenges in controlling prostheses is that a practical prosthesis will only have sensors on itself instead of on the full bipedal system as in the case of robots. As a result, the prosthesis controller will only have information about its own state, which potentially makes feedback linearization more challenging. A related problem arises in the field of multi-machine power systems. Similar to the human-prosthesis system, the dynamics of each subsystem are both nonlinear and coupled, although the structure of the equations are very different between the two fields [11]. Localized, feedback-linearizing controllers have been developed specifically for power systems to reduce the system dimension [12]. For a prosthesis controller, the challenge is in deriving the feedback linearizing controller for a coupled mechanical, rather than electrical [12], system. Because the prosthesis is attached to the human via a socket, the human and prosthesis interact through the socket interaction force. This coupling force represents the effects of one subsystem on the other, and can be used to account for the human’s dynamics in the prosthesis controller. In hardware, the socket interaction force can be measured, but equations to calculate it in simulation must be derived.

Pre-clinical work has shown that a powered above-knee prosthesis controlled with an HZD-like controller during stance and an impedance-based controller during swing allows amputees to walk at a variety of speeds and ground slopes [13], [14]. That work did not generalize the feedback linearizing controller to the prosthesis swing phase or, to allow for more realistic modeling, to the human subsystem. The feasibility of the controller was verified in simulation using a symmetric biped with a passive hip joint walking down a very shallow slope, effectively simulating a bilateral amputee walking down a ramp. Most amputees still have

\*This work was supported by the National Institute of Child Health & Human Development of the NIH under Award Number DP2HD080349. The content is solely the responsibility of the authors and does not necessarily represent the official views of the NIH. R. D. Gregg holds a Career Award at the Scientific Interface from the Burroughs Wellcome Fund.

<sup>1</sup>Anne Martin is with the Department of Mechanical Engineering, University of Texas at Dallas, Richardson, TX 75080, USA [Anne.Martin@utdallas.edu](mailto:Anne.Martin@utdallas.edu)

<sup>2</sup>Robert Gregg is with the Departments of Bioengineering and Mechanical Engineering, University of Texas at Dallas, Richardson, TX 75080, USA [rgregg@utdallas.edu](mailto:rgregg@utdallas.edu)

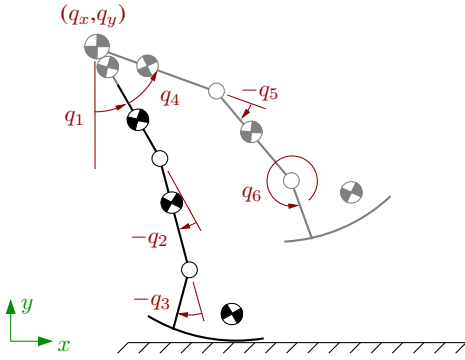


Fig. 1. Schematic of the above-knee amputee model. The prosthesis is shown in black and the human is shown in gray. The generalized coordinates are shown in red.

one intact leg, so an asymmetric model would be more appropriate. Further, the amputee retains direct control of his/her intact joints, and this control cannot be fully captured in simulation using a passive hip joint. The work also did not make use of the reduced order system to develop an analytical metric of stability, in part because the output functions were not hybrid invariant.

The present work extends the modeling and control methods needed to formally develop hybrid invariant prosthesis controllers for the entire stride and to predictively test these controllers in simulation. Specifically, using an asymmetric biped, this work

- derives the equations for the socket interaction force between the human and prosthesis,
- shows how to construct feedback linearizing controllers for both the human and prosthesis using only information available to each subsystem, and
- develops an analytic metric of stability using a reduced order system.

The results are illustrated using a model of an above-knee amputee wearing a powered prosthesis.

## II. MODEL

### A. Physical Model

The full planar model of the unilateral above-knee amputee consists of seven leg segments plus a point mass at the hip to represent the upper body (Fig. 1). To account for the lack of information transmitted between the human and prosthesis, the full model can be divided into a prosthesis subsystem and a human subsystem [14]. The prosthesis subsystem consists of the prosthetic thigh, shank, and foot. The human subsystem consists of the contralateral thigh, shank, and foot, the residual thigh on the amputated side, and the point mass at the hip. It is assumed that the prosthetic thigh and residual stump are rigidly attached. Rather than model all of the DoF of the foot, the function of the foot and ankle is modeled using a circular foot plus an ankle joint [10] to capture both the center of pressure movement [15], [16] and the positive work performed at the stance ankle [17].

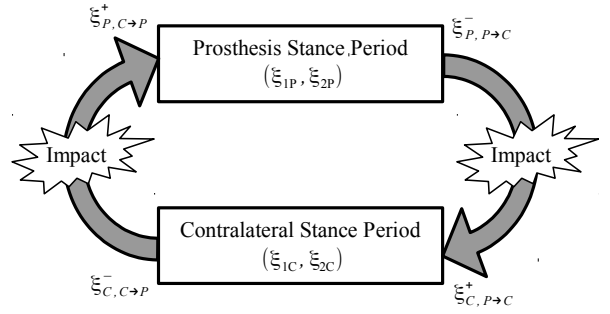


Fig. 2. The periodic gait. The  $\xi$  terms are the zero dynamics coordinates used for the reduced system (Sec. IV). For simulation, a stride starts just after the transition from contralateral stance to prosthesis stance and proceeds through the prosthesis stance period, an impact event, the contralateral stance period and a second impact.

Because the biped is assumed to roll without slip, one DoF is unactuated. The remaining joints are assumed to have ideal actuators. Dividing the torques by subsystem gives  $u_P = [u_2 \ u_3]^T$  for the prosthesis and  $u_H = [u_4 \ u_5 \ u_6]^T$  for the human. Because the prosthesis is rigidly attached to the residual limb, forces and moments are transmitted through this interface and provide an indirect measure of the motion of both subsystems via the socket interaction force  $F = [F_x \ F_y \ F_M]^T$ . The leg in stance also experiences horizontal and vertical ground reaction forces (GRF)  $G = [G_x \ G_y]^T$ . There is no moment at the foot-ground interface due to the curved foot. Similar to the torques, each subsystem has its own set of generalized coordinates. In general, each subsystem's generalized coordinates should be the relative angles of its actuated joints, the absolute angle of the unactuated DoF, and the Cartesian coordinates of a fixed point on the biped. For the model in this paper (Fig. 1),  $q_1$  is the absolute angle, and the fixed point is the hip position  $(q_x, q_y)$ . The actuated joint angles are  $q_2$ - $q_6$ . Thus, the generalized coordinates for the prosthesis are  $q_P = [q_1 \ q_2 \ q_3 \ q_x \ q_y]^T$  and the generalized coordinates for the human are  $q_H = [q_1 \ q_4 \ q_5 \ q_6 \ q_x \ q_y]^T$ .

Each stride is modeled using four distinct periods (Fig. 2). The two stance periods are modeled with continuous, second-order differential equations, and the two instantaneous impact periods are modeled using an algebraic mapping that relates the state of the biped at the instant before impact to the state at the instant after impact. The stance leg switches during the impact period.

### B. Single Support Periods

The equations of motion (EoM) during the single support period for a subsystem can be written as

$$M_i \ddot{q}_i + C_i \dot{q}_i + N_i - E_{ij}^T G = B_i u_i + J_i^T F. \quad (1)$$

Throughout this paper, the subscript  $i$  indicates which subsystem the term is for, with  $P$  indicating the prosthesis subsystem and  $H$  indicating the human subsystem. The subscript  $j$  indicates which leg is in stance, with  $P$  indicating the prosthesis and  $C$  indicating the contralateral leg.  $M_i$

is the  $\mathcal{N}_i \times \mathcal{N}_i$  inertia matrix,  $C_i$  is the  $\mathcal{N}_i \times \mathcal{N}_i$  matrix containing the centripetal and Coriolis terms,  $N_i$  is the  $\mathcal{N}_i \times 1$  gravity vector,  $E_{ij}$  is a  $2 \times \mathcal{N}_i$  constraint matrix,  $B_i$  is the  $\mathcal{N}_i \times \mathcal{M}_i$  matrix relating the input torques to the generalized coordinates, and  $J_i$  is the  $3 \times \mathcal{N}_i$  Jacobian matrix relating the socket interaction forces to the generalized coordinates. For the above-knee prosthesis subsystem, the number of the generalized coordinates is  $\mathcal{N}_P = 5$  and the number of input torques is  $\mathcal{M}_P = 2$ . For the above-knee human amputee subsystem, the number of the generalized coordinates is  $\mathcal{N}_H = 6$  and the number of input torques is  $\mathcal{M}_H = 3$ . Except for the constraint matrix  $E_{ij}$ , all matrices are identical regardless of which leg is in stance. Because the constraint matrix is used to specify how the biped is attached to the ground, it is only defined when the subsystem is in stance and is set to zero during the swing phase.

To attach the biped to the ground, the constraint equation

$$E_{ij}\dot{q}_i = 0 \quad (2)$$

is used [18]. Solving the EoM (Eq. 1) for  $\ddot{q}_i$ , substituting it into the derivative of Eq. 2, and solving for the GRF gives

$$G = \widehat{\lambda}_{ij} + \widetilde{\lambda}_{ij}u_i + \bar{\lambda}_{ij}F \quad (3)$$

where

$$\begin{aligned} \widehat{\lambda}_{ij} &= W_{ij}(E_{ij}M_i^{-1}(C_i\dot{q}_i + N_i) - \dot{E}_{ij}\dot{q}_i), \\ \widetilde{\lambda}_{ij} &= -W_{ij}E_{ij}M_i^{-1}B_i, \\ \bar{\lambda}_{ij} &= -W_{ij}E_{ij}M_i^{-1}J_i^T, \\ W_{ij} &= (E_{ij}M_i^{-1}E_{ij}^T)^{-1}. \end{aligned}$$

Substituting the GRF (Eq. 3) back into the EoM (Eq. 1) and solving for  $\ddot{q}_i$  gives

$$\begin{aligned} \ddot{q}_i &= M_i^{-1}(-C_i\dot{q}_i - N_i + E_{ij}^T(\widehat{\lambda}_{ij} + \widetilde{\lambda}_{ij}u_i + \bar{\lambda}_{ij}F)) \\ &\quad + M_i^{-1}B_iu_i + M_i^{-1}J_i^TF. \end{aligned} \quad (4)$$

Eq. 4 defines the motion of subsystem  $i$  when leg  $j$  is in stance. In anticipation of the controller design (Sec. III), Eq. 4 can also be written as a first-order ODE:

$$\dot{x}_i = f_{ij}(x_i) + g_{ij}(x_i)u_i + p_{ij}(x_i)F, \quad (5)$$

where

$$\begin{aligned} x_i &= [q_i^T \dot{q}_i^T]^T, \\ f_{ij}(x) &= \begin{bmatrix} \dot{q}_i \\ -M_i^{-1}(C_i\dot{q}_i + N_i - E_{ij}^T\widehat{\lambda}_{ij}) \end{bmatrix}, \\ g_{ij}(x) &= \begin{bmatrix} 0 \\ M_i^{-1}(E_{ij}^T\widetilde{\lambda}_{ij} + B_i) \end{bmatrix}, \\ p_{ij}(x) &= \begin{bmatrix} 0 \\ M_i^{-1}(E_{ij}^T\bar{\lambda}_i + J_i^T) \end{bmatrix}. \end{aligned}$$

### C. Impact Periods

To model the impact periods, an algebraic mapping is used. Because the configuration of the biped is assumed to remain constant over the impact period, the position portion of the impact map is trivial:

$$q_{i,k}^+ = q_{i,k}^-, \quad (6)$$

where the superscript ‘-’ refers to the instant before impact, the superscript ‘+’ refers to the instant after impact,  $k = P \rightarrow C$  indicates that the transition is from the prosthesis stance period to the contralateral stance period, and  $k = C \rightarrow P$  indicates that the transition is from the contralateral stance period to the prosthesis stance period. To find the velocity portion of the impact map, the EoM (Eq. 1) are integrated over the instantaneous duration of impact [8], [9]. To fix the biped to the ground, the post-impact constraint equation (Eq. 2) is used. Because the human and prosthesis subsystems share some generalized coordinates, the motion of these shared DoF must be the same for both subsystems which can be enforced using

$$S_P\dot{q}_P = S_H\dot{q}_H, \quad (7)$$

where

$$\begin{aligned} S_P &= \begin{bmatrix} 1 & 0 & 0 & 0 & 0 \\ 0 & 0 & 0 & 1 & 0 \\ 0 & 0 & 0 & 0 & 1 \end{bmatrix}, \\ S_H &= \begin{bmatrix} 1 & 0 & 0 & 0 & 0 & 0 \\ 0 & 0 & 0 & 0 & 1 & 0 \\ 0 & 0 & 0 & 0 & 0 & 1 \end{bmatrix}. \end{aligned}$$

This results in a square linear system in which the unknowns are the post-impact velocities for both subsystems, the ground reaction impulse and the socket interaction impulse. Solving for the post-impact velocities and socket interaction impulse  $\mathcal{F}$  results in

$$\dot{q}_{i,k}^+ = A_{i,k}\dot{q}_{i,k}^- + \Lambda_{i,k}\mathcal{F}, \quad (8)$$

$$\begin{aligned} \mathcal{F} &= (S_P\Lambda_{P,k} - S_H\Lambda_{H,k})^{-1} \\ &\quad \cdot (S_H A_{H,k}\dot{q}_{H,k}^- - S_P A_{P,k}\dot{q}_{P,k}^-), \end{aligned} \quad (9)$$

where

$$\begin{aligned} A_{P,P \rightarrow C} &= I_{5 \times 5}, & A_{H,C \rightarrow P} &= I_{6 \times 6}, \\ \Lambda_{P,P \rightarrow C} &= M_P^{-1}J_P^T, & \Lambda_{H,C \rightarrow P} &= M_H^{-1}J_H^T, \\ A_{H,P \rightarrow C} &= I_{6 \times 6} - M_H^{-1}E_{HC}^T(E_{HC}M_H^{-1}E_{HC}^T)^{-1}E_{HC}, \\ \Lambda_{H,P \rightarrow C} &= M_H^{-1}(J_H^T - E_{HC}^T(E_{HC}M_H^{-1}E_{HC}^T)^{-1} \\ &\quad \cdot E_{HC}M_H^{-1}J_H^T), \\ A_{P,C \rightarrow P} &= I_{5 \times 5} - M_P^{-1}E_{PP}^T(E_{PP}M_P^{-1}E_{PP}^T)^{-1}E_{PP}, \\ \Lambda_{P,C \rightarrow P} &= M_P^{-1}(J_P^T - E_{PP}^T(E_{PP}M_P^{-1}E_{PP}^T)^{-1} \\ &\quad \cdot E_{PP}M_P^{-1}J_P^T). \end{aligned}$$

### III. CONTROL

To control both the prosthesis and the human, feedback linearization is used [8], [19]. With the exception of the stability analysis (Sec. IV), the results for the prosthesis are independent of the form of the human controller. To account for the lack of information transmitted between the human and prosthesis, the prosthesis controller only uses information that could be collected by on-board sensors, i.e., the prosthesis generalized coordinates and associated derivatives and the socket interaction force [14]. Further, it is assumed that the prosthesis either estimates (using Eq. 3) or measures the GRF on the prosthetic side (e.g. [13]). Similarly, since the

human cannot directly sense the prosthesis state, the human controller only uses information about the human generalized coordinates and associated derivatives, the socket interaction force, and the GRF on the contralateral side.

To perform feedback linearization, the desired motion of the actuated angles are encoded in output functions to be zeroed [8]:

$$y_{ij} = h_{ij}(q_i), \quad (10)$$

where  $h_{ij}$  is a vector-valued function of dimension  $\mathcal{M}_i$ .  $h_{ij}$  is a function of configuration only since the motion is parametrized using a kinematic phase variable. Differentiating Eq. 10 twice and substituting in the EoM (Eq. 5) for  $\ddot{q}_i$  gives the output dynamics

$$\ddot{y}_{ij} = L_{f_{ij}}^2 h_{ij} + L_{g_{ij}} L_{f_{ij}} h_{ij} \cdot u_i + L_{p_{ij}} L_{f_{ij}} h_{ij} \cdot F, \quad (11)$$

where standard Lie derivative notation [19] has been used and the terms are given by

$$\begin{aligned} L_{f_{ij}}^2 h_{ij} &= \frac{\partial}{\partial q_i} \left( \frac{\partial h_{ij}}{\partial q_i} \dot{q}_i \right) \dot{q}_i \\ &\quad - \frac{\partial h_{ij}}{\partial q_i} M_i^{-1} (C_i \dot{q}_i + N_i - E_{ij}^T \tilde{\lambda}_{ij}), \\ L_{g_{ij}} L_{f_{ij}} h_{ij} &= \frac{\partial h_{ij}}{\partial q_i} M_i^{-1} (E_{ij}^T \tilde{\lambda}_{ij} + B_i), \\ L_{p_{ij}} L_{f_{ij}} h_{ij} &= \frac{\partial h_{ij}}{\partial q_i} M_i^{-1} (E_{ij}^T \tilde{\lambda}_{ij} + J_i^T). \end{aligned}$$

To cancel the nonlinearities in the output dynamics, set  $\ddot{y}_{ij} = v_{ij}$  where  $v_{ij}$  is a stabilizing controller and solve for the input torques:

$$u_i = \alpha_{ij} + \beta_{ij} \cdot F, \quad (12)$$

where

$$\begin{aligned} \alpha_{ij} &= L_{g_{ij}} L_{f_{ij}} h_{ij}^{-1} (v_{ij} - L_{f_{ij}}^2 h_{ij}), \\ \beta_{ij} &= -L_{g_{ij}} L_{f_{ij}} h_{ij}^{-1} \cdot L_{p_{ij}} L_{f_{ij}} h_{ij}. \end{aligned}$$

Eq. 12 defines the input torques required to cancel the nonlinearities in the EoM and zero the tracking errors for subsystem  $i$  when leg  $j$  is in stance. The input torque for subsystem  $i$  only depends on quantities that subsystem  $i$  can measure.

Eq. 12 combined with sensor measurements can be used to find the input in hardware. However, for simulation, the socket interaction force  $F$  needs to be determined. Substituting the EoM (Eq. 4) and torques (Eq. 12) into the derivative of the matching equation (Eq. 7) and rearranging gives

$$F = F_{den,j}^{-1} \cdot F_{num,j}, \quad (13)$$

where

$$\begin{aligned} F_{den,j} &= S_P M_P^{-1} (B_P \beta_{Pj} + J_P^T \\ &\quad + E_{Pj}^T (\tilde{\lambda}_{Pj} \beta_{Pj} + \bar{\lambda}_{Pj})) \\ &\quad - S_H M_H^{-1} (B_H \beta_{Hj} + J_H^T \\ &\quad + E_{Hj}^T (\tilde{\lambda}_{Hj} \beta_{Hj} + \bar{\lambda}_{Hj})), \end{aligned}$$

$$\begin{aligned} F_{num,j} &= S_H M_H^{-1} (-C_H \dot{q}_H - N_H + B_H \alpha_{Hj} \\ &\quad + E_{Hj}^T (\tilde{\lambda}_{Hj} + \tilde{\lambda}_{Hj} \alpha_{Hj})) \\ &\quad - S_P M_P^{-1} (-C_P \dot{q}_P - N_P + B_P \alpha_{Pj} \\ &\quad + E_{Pj}^T (\tilde{\lambda}_{Pj} + \tilde{\lambda}_{Pj} \alpha_{Pj})). \end{aligned}$$

The socket force is linear in velocity, which will be important when analyzing stability (Sec. IV).

To implement feedback linearization, output functions must be defined to characterize the desired kinematics of the actuated joints as a function of the phase variable. A total of four (vector-valued) output functions are required because each subsystem  $i$  requires an output function for each stance period  $j$  (Fig. 2). To perform the stability analysis (Sec. IV), the gait must be hybrid invariant, i.e., the output functions must respect the impact dynamics (Eqs. 6 and 8). If the desired motion of the full system is known and the output functions are defined using Bézier polynomials, conditions to ensure hybrid invariance can be derived [8].

#### IV. STABILITY

Since it is assumed that unilateral amputee gait is two-step periodic, stability can be evaluated using the method of Poincaré. The instant before the transition to the prosthesis stance period is chosen as the Poincaré section. To reduce the dimension of the Poincaré map, a nonlinear coordinate transformation can be applied to the system to render most coordinates equal to zero if the output functions are hybrid invariant [8]. For a planar, symmetric biped with full knowledge of its state, it is possible to find an analytic orbital stability criteria. The goal is to show that this is also possible for the coupled human plus prosthesis system.

There are a total of six independent DoF for the full human plus prosthesis system, which means there are a total of twelve independent coordinates (6 position and 6 velocity). The position of the hip is a function of the joint angles and not independent because the biped is assumed to roll without slip. For reasons that will be explained later, the transformation between the original, nonlinear EoM and the new, feedback linearized system will only be for the twelve independent coordinates. The first 10 coordinates in the new system are given by

$$\eta_{1j} = \begin{bmatrix} y_{Pj} \\ y_{Hj} \end{bmatrix} = \begin{bmatrix} h_{Pj}(q_P) \\ h_{Hj}(q_H) \end{bmatrix}, \quad (14)$$

$$\eta_{2j} = \begin{bmatrix} \dot{y}_{Pj} \\ \dot{y}_{Hj} \end{bmatrix} = \begin{bmatrix} \frac{\partial h_{Pj}}{\partial q_P} \dot{q}_P \\ \frac{\partial h_{Hj}}{\partial q_H} \dot{q}_H \end{bmatrix}. \quad (15)$$

Because  $y_{ij}$  is the output for subsystem  $i$  when leg  $j$  is in stance,  $\eta_{1j}$  and  $\eta_{2j}$  represent the error in configuration and velocity for the entire system. For a hybrid invariant gait on the periodic orbit,  $\eta_{1j}$  and  $\eta_{2j}$  equal zero. Since the goal is to design a stable controller for the prosthesis, a logical choice for the final two coordinates is [8]

$$\xi_{1j} = \theta_{Pj}(q_P), \quad (16)$$

$$\xi_{2j} = \dot{M}_{Pj} \dot{q}_P, \quad (17)$$

where  $\theta_{Pj}$  is the monotonically increasing phase variable for the prosthesis that captures the motion of the unactuated angle, and  $\check{M}_{Pj1}$  is the row of the prosthesis inertia matrix corresponding to the unactuated DoF, where the inertia matrix is found using only the prosthesis joint angles  $\check{q}_P = [q_1 \ q_2 \ q_3]^T$ . Without loss of generality, assume that the unactuated angle is  $q_1$ . Since the human motion does not directly appear in the zero dynamics coordinates ( $\xi_{1j}$  and  $\xi_{2j}$ ), there is the possibility that the orbital stability will only depend on the prosthesis and the motion of the human can be ignored. This is advantageous because the designer has direct control over the prosthesis controller whereas human motion can be difficult to predict. Differentiating Eqs. 14-17 to obtain the EoM in the transformed system yields

$$\dot{\eta}_{1j} = \eta_{2j} \quad (18)$$

$$\dot{\eta}_{2j} = \begin{bmatrix} v_{Pj} \\ v_{Hj} \end{bmatrix} \quad (19)$$

$$\dot{\xi}_{1j} = \frac{\partial \theta_{Pj}}{\partial q_P} \dot{q}_P \quad (20)$$

$$\dot{\xi}_{2j} = \check{q}_P^T \frac{\partial \check{M}_{Pj1}^T}{\partial \check{q}_P} \dot{q}_P - \check{C}_{Pj1} \dot{q}_P - \check{N}_{Pj1} + \check{J}_{Pj1}^T F, \quad (21)$$

where  $\check{C}_{Pj1}$  is the top row of the centripetal and Coriolis matrix,  $\check{N}_{Pj1}$  is the top entry in the gravity vector and  $\check{J}_{Pj1}^T$  is the top row of transpose of the Jacobian matrix that relates the socket interaction forces to the generalized coordinates, all for the prosthesis and found using  $\check{q}_P$ . Notice that the new system can be viewed as a linear upper system that only depends on  $\eta_{1j}$  and  $\eta_{2j}$  and a passive, nonlinear lower system of dimension two that depends on all of the prosthesis coordinates. Note that if the position of the hip was included in the transformation between the original, nonlinear EoM and the new, feedback linearized system, then the dimension of the lower system would be four and it may no longer be passive. Both the increased dimension and the non-passive nature of the lower system would prevent the determination of an analytical stability metric for orbital stability.

Since  $\dot{\eta}_{1j}$  and  $\dot{\eta}_{2j}$  are zero on the periodic orbit,  $\dot{\xi}_{1j}$  and  $\dot{\xi}_{2j}$  determine the orbital stability. For a symmetric biped with full knowledge of its state, Eqs. 20 and 21 can be combined into a single, first order linear differential equation in which the independent variable is  $\xi_1$ . This equation can then be integrated over a periodic step and the impact map applied to obtain an analytic expression for the Poincaré return map [8], [9]. To formulate the first order differential equation, the fact that  $\dot{\xi}_2$  is purely quadratic in velocity is exploited. However, when  $\xi_{2j}$  is chosen as in Eq. 17,  $\dot{\xi}_{2j}$  has a linear velocity term due to the socket interaction force (Eq. 13). As a result, it is no longer possible to formulate a linear differential equation, and there is no obvious analytic solution for the nonlinear differential equation.

While it is certainly possible to compute the Poincaré return map numerically if  $\xi_{2j}$  is defined using Eq. 17, there is an additional issue. When the prosthesis is in stance, it is possible to formulate its EoM without including the hip position in the generalized coordinates because the prosthesis

can be considered fixed to the ground. When the prosthesis is in swing, however, the hip position must be included in the generalized coordinates. As a result, either the hip state has to be included in the nonlinear transformation, or the hip state must be expressed as a function of the human state, which leads to  $\xi_{2C}$  being a function of both the human and prosthesis states. Neither option is appealing, the first because it increases the dimension of the zero dynamics and the second because stability no longer just depends on the prosthesis. In addition, regardless of which foot is in stance,  $\xi_{2j}$  is a function of both the human state and the prosthesis state due to the socket interaction forces. Taken together, it appears there is no advantage in using just the prosthesis to define  $\xi_{2j}$ . This is not a surprising result because the motion of the prosthesis is influenced by the motion of the human, so it is reasonable for the stability to depend on both the prosthesis and the human.

Since the orbital stability depends on both the human and prosthesis, it is easiest to combine the two subsystems and evaluate them together. Thus,  $\xi_{2j}$  is chosen as

$$\xi_{2j} = D_{j1} \dot{q}, \quad (22)$$

where  $D_{j1}$  is the top row of the inertia matrix for the full human plus prosthesis system and  $q = [q_1 \ q_2 \ q_3 \ q_4 \ q_5 \ q_6]^T$ . Again, without loss of generality, the unactuated angle is  $q_1$ . Note that  $D_{P1} \neq D_{C1}$  because the inertia matrix includes the ground contact constraint. Choosing  $\xi_{2j}$  as in Eq. 22 assumes full knowledge of the biped's state, so the methods to evaluate stability in [8] and [9] can be used. The controllers remain independent even though the stability analysis depends on the motion of both subsystems.

Using Eqs. 14-16 and 22 as the coordinates for the transformed system, the procedure in [9] is followed to obtain analytic equations relating the state of the biped just after impact to the state just before the next impact. Briefly, the equations for the zero dynamics (Eqs. 16 and 22) are combined into a scalar, linear, first-order differential equation for each stance period and those equations are integrated over the corresponding stance period to obtain

$$\zeta_{P,P \rightarrow C}^- = b_{1P} \left( b_{2P} + \zeta_{P,C \rightarrow P}^+ \right) \quad (23)$$

for the prosthesis stance period and

$$\zeta_{C,C \rightarrow P}^- = b_{1C} \left( b_{2C} + \zeta_{C,P \rightarrow C}^+ \right) \quad (24)$$

for the contralateral stance period. The terms are given by

$$\begin{aligned} \zeta_{j,k} &= \frac{1}{2} \xi_{2j}^2, & b_{1j} &= e^{-c_j(\xi_{1j}^-)}, \\ b_{2j} &= - \int_{\xi_{1j}^+}^{\xi_{1j}^-} e^{c_j(\tau)} \frac{N_{j1}(\tau)}{\frac{\partial \theta_{Pj}(q)}{\partial q} \Big|_{\tau} \cdot \phi_j(\tau)} d\tau, \\ c_j(\xi_{1j}) &= - \int_{\xi_{1j}^+}^{\xi_{1j}^-} \frac{\phi_j^T(\tau) \cdot \frac{\partial D_j(q)}{\partial q_1} \Big|_{\tau} \cdot \phi_j(\tau)}{\frac{\partial \theta_{Pj}(q)}{\partial q} \Big|_{\tau} \cdot \phi_j(\tau)} d\tau, \\ \phi_j(\xi_{1j}) &= \begin{bmatrix} \frac{\partial h_{Pj}}{\partial q} \Big|_{\xi_{ij}} \\ \frac{\partial h_{Hj}}{\partial q} \Big|_{\xi_{ij}} \\ D_{j1}(\xi_{1j}) \end{bmatrix}^{-1} \begin{bmatrix} 0_{5 \times 1} \\ 1 \end{bmatrix}, \end{aligned}$$

where  $N_{j1}$  is the top row of the gravity vector for the full biped found using  $q$ ,  $\xi_{1P}^- = \xi_{1P,P \rightarrow C}^-$  is the value of  $\xi_{1P}$  evaluated just before the transition from the prosthesis stance period to contralateral stance period,  $\xi_{1C}^- = \xi_{1C,C \rightarrow P}^-$  is the value of  $\xi_{1C}$  evaluated just before the transition from the contralateral stance period to prosthesis stance period,  $\xi_{1C}^+ = \xi_{1C,P \rightarrow C}^+$  is the value of  $\xi_{1C}$  evaluated just after the transition from the prosthesis stance period to contralateral stance period, and  $\xi_{1P}^+ = \xi_{1P,C \rightarrow P}^+$  is the value of  $\xi_{1P}$  evaluated just after the transition from the contralateral stance period to prosthesis stance period (Fig. 2). To convert between joint angles and  $\xi_{1j}$ , use

$$\begin{bmatrix} 0_{5 \times 1} \\ \xi_{1j} \end{bmatrix} = \begin{bmatrix} h_{Pj}(q) \\ h_{Hj}(q) \\ \theta_{Pj}(q) \end{bmatrix}. \quad (25)$$

To find the Poincaré return map, Eqs. 23 and 24 can be related using the impact map for the full system:

$$\zeta_{C,P \rightarrow C}^+ = \delta_{P \rightarrow C}^2 \zeta_{P,P \rightarrow C}^-, \quad (26)$$

$$\zeta_{P,C \rightarrow P}^+ = \delta_{C \rightarrow P}^2 \zeta_{C,C \rightarrow P}^-, \quad (27)$$

where

$$\begin{aligned} \delta_{P \rightarrow C} &= D_{C1} A_{P \rightarrow C} \phi_P, \\ \delta_{C \rightarrow P} &= D_{P1} A_{C \rightarrow P} \phi_C, \\ A_k &= \Lambda_{11} - \Lambda_{12} E_{1,k}, \\ \Lambda_k &= I_{8 \times 8} - M_e^{-1} E_{e,k}^T (E_{e,k} M_e^{-1} E_{e,k}^T)^{-1} E_{e,k} \\ &= \begin{bmatrix} \Lambda_{11} & \Lambda_{12} \\ \Lambda_{21} & \Lambda_{22} \end{bmatrix}, \end{aligned}$$

$M_e$  is the inertia matrix for the whole biped when the generalized coordinates are the joint angles plus the hip position,  $E_{e,k}$  is the constraint matrix used to attach the biped to the ground when the generalized coordinates are the joint angles plus the hip position,  $\Lambda_{11}$  is a  $6 \times 6$  matrix, and  $\Lambda_{12}$  is a  $6 \times 2$  matrix. The  $2 \times 6$  matrix  $E_{1,k}$  transforms the pre-impact single support joint velocities into the pre-impact hip velocities. When  $k = P \rightarrow C$ ,  $E_{e,P \rightarrow C}$  is used to attach the contralateral foot to the ground and  $E_{1,P \rightarrow C}$  is used to attach the prosthesis to the ground. When  $k = C \rightarrow P$ ,  $E_{e,C \rightarrow P}$  is used to attach the prosthesis to the ground and  $E_{1,C \rightarrow P}$  is used to attach the contralateral foot to the ground. All terms are evaluated using the angles at impact. Substituting Eqs. 26 and 27 into Eqs. 23 and 24 and solving for the state at the end of the contralateral stance period gives

$$\zeta_{C,C \rightarrow P}^- = b_{1C} \left( b_{2C} + \delta_{P \rightarrow C}^2 b_{1P} \left( b_{2P} + \delta_{C \rightarrow P}^2 \zeta_{C,C \rightarrow P}^- \right) \right). \quad (28)$$

Eq. 28 is the Poincaré map. To check stability, it can be differentiated with respect to  $\zeta_{C,C \rightarrow P}^-$  to find the stability criterion:

$$0 < b_{1P} b_{1C} \delta_{P \rightarrow C}^2 \delta_{C \rightarrow P}^2 < 1. \quad (29)$$

All four terms depend on the motion of both the human and the prosthesis. The stability criterion serves as a nonlinear constraint on the human and prosthesis output functions used to define a gait [20] because a usable gait must be stable. If

TABLE I  
TEMPORAL GAIT PROPERTIES

	Prosthesis Stance	Contralateral Stance
Step Length (m)	0.719	0.723
Step Duration (s)	0.448	0.434
Speed (m/s)	1.604	1.666

the zero dynamics are stable, the stability of the full system can be easily proven if PD controllers are used for the output feedback controller  $v_{ij}$  in Eq. 12 [21].

## V. EXAMPLE

To demonstrate the controller, simulations were conducted (Fig. 3). The model has a leg length of 90.6 cm and a total mass of 69.3 kg. The mass of the prosthesis is 5.7 kg, which is approximately the same as the physiological leg that it replaces. The length and mass parameters for the prosthesis were based on the physical properties of the powered above-knee prosthesis currently being built at the University of Texas at Dallas. The output functions for both the human and prosthesis controllers were chosen to approximate healthy human gait, although no effort was made to impose either symmetry or asymmetry on the resulting gait. The phase variable for both the human and prosthesis controllers was chosen as the horizontal hip position. The resulting orbital stability metric is 0.860, which is between 0 and 1, so the gait is stable. Since the gait is stable, the amputee does not have to react to or compensate for perturbations on behalf of the prosthesis, which could reduce both the physical and mental effort required for gait. Due to the asymmetries between the amputated and contralateral legs, the gait is two-step periodic as expected (Table I, Figs. 3 and 4). When started on the periodic orbit, errors are on the order of the simulation's numerical precision (approximately  $10^{-5}$  rad for position and  $10^{-4}$  rad/s for velocity), demonstrating that the gait is indeed stable and hybrid invariant. As further proof that the gait is stable, if the simulation's initial conditions are not exactly on the periodic orbit, the biped converges to the orbit over many steps (Fig. 4).

## VI. CONCLUSIONS

Using only information that can be measured with on-board sensors, it is possible to perform feedback linearizing control on a powered prostheses. Similarly, it is possible to model the human joint control using feedback linearization assuming the human does not have direct knowledge of what the prosthesis is doing. If the desired motion of both the human and prosthesis is known or can be accurately estimated, it is possible to design controllers that are hybrid invariant and provably stable. Work is currently being conducted to determine how to guarantee hybrid invariance and orbital stability even in the presence of unknown human motions.

## REFERENCES

- [1] P. DeVita, J. Helseth, and T. Hortobagyi, "Muscles do more positive than negative work in human locomotion," *J. Exp. Biol.*, vol. 210, no. 19, pp. 3361–73, 2007.

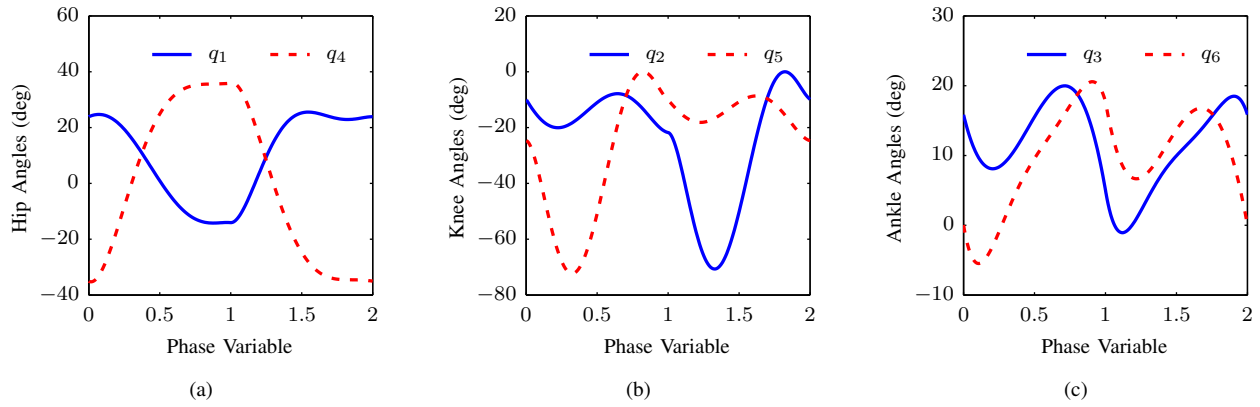


Fig. 3. (a) Hip, (b) knee, and (c) ankle angles vs. the normalized phase variable. The prosthesis stance period occurs from 0 to 1 and the contralateral stance period occurs from 1 to 2.

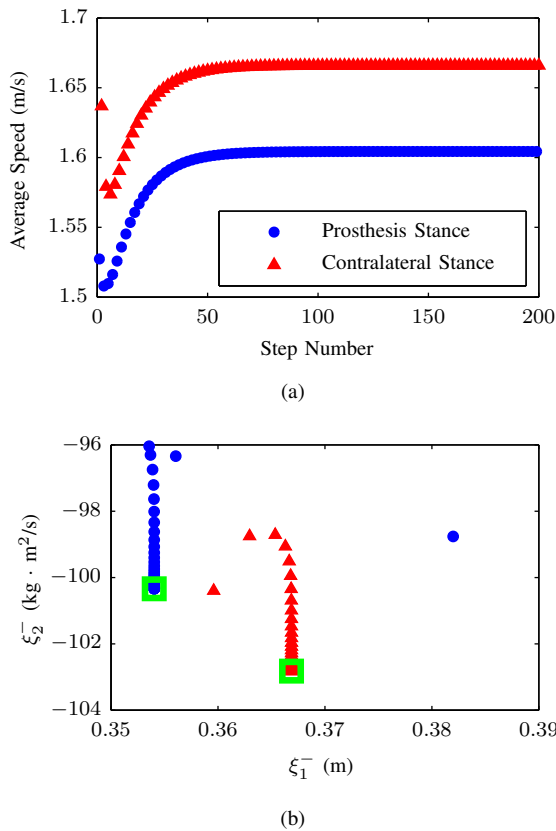


Fig. 4. (a) The average speed per step. (b) The zero dynamics (given by Eqs. 16 and 22) just before impact. For the zero dynamics, the equilibrium points are indicated with the green squares. The simulation did not start on the periodic orbit but clearly converged to it.

[2] F. Sup, A. Bohara, and M. Goldfarb, "Design and control of a powered transfemoral prosthesis," *Int. J. Robot. Res.*, vol. 27, no. 2, pp. 263–73, 2008.

[3] M. F. Eilenberg, H. Geyer, and H. Herr, "Control of a powered ankle-foot prosthesis based on a neuromuscular model," *IEEE Trans. Neural Syst. Rehabil. Eng.*, vol. 18, no. 2, pp. 164–73, 2010.

[4] A. M. Simon, K. A. Ingraham, N. P. Fey, S. B. Finucane, R. D. Lipschutz, A. J. Young, and L. J. Hargrove, "Configuring a powered knee and ankle prosthesis for transfemoral amputees within five specific ambulation modes," *PLoS ONE*, vol. 9, no. 6, p. e99387, 2014.

[5] M. A. Holgate, T. G. Sugar, and A. W. Bohler, "A novel control algorithm for wearable robotics using phase plane invariants," in *2009 IEEE Int. Conf. on Robot. Autom. (ICRA)*, May 2009, pp. 3845–50.

[6] R. D. Gregg, E. J. Rouse, L. J. Hargrove, and J. W. Sensinger, "Evidence for a time-invariant phase variable in human ankle control," *PLoS ONE*, vol. 9, no. 2, p. e89163, 2014.

[7] D. J. Villarreal and R. D. Gregg, "A survey of phase variable candidates of human locomotion," in *IEEE Eng. Med. Bio.*, Chicago, IL, Aug. 2014.

[8] E. R. Westervelt, J. W. Grizzle, C. Chevallereau, J. H. Choi, and B. Morris, *Feedback Control of Dynamic Bipedal Robot Locomotion*. CRC Press, 2007.

[9] A. E. Martin, D. C. Post, and J. P. Schmedeler, "Design and experimental implementation of a hybrid zero dynamics-based controller for planar bipeds with curved feet," *Int. J. Robot. Res.*, vol. 33, no. 7, pp. 988–1005, 2014.

[10] A. E. Martin and J. P. Schmedeler, "Predicting human walking gaits with a simple planar model," *J. Biomech.*, vol. 47, no. 6, pp. 1416–21, 2014.

[11] Y. Wang, G. Guo, and D. J. Hill, "Robust decentralized nonlinear controller design for multimachine power systems," *Automatica*, vol. 33, no. 97, pp. 1725–33, 1997.

[12] E. De Tuglie, S. M. Iannone, and F. Torelli, "Feedback-linearization and feedback-feedforward decentralized control for multimachine power system," *Electr. Pow. Syst. Res.*, vol. 78, pp. 382–91, 2008.

[13] R. D. Gregg, T. Lenzi, L. J. Hargrove, and J. W. Sensinger, "Virtual constraint control of a powered prosthetic leg: From simulation to experiments with transfemoral amputees," *IEEE T. Robot.*, vol. 30, no. 6, pp. 1455–71, 2014.

[14] R. D. Gregg and J. W. Sensinger, "Biomimetic virtual constraint control of a transfemoral powered prosthetic leg," in *Amer. Control Conf.*, 2013, pp. 5702–8.

[15] A. H. Hansen, D. S. Childress, and E. H. Knox, "Roll-over shapes of human locomotor systems: Effects of walking speed," *Clin. Biomech.*, vol. 19, no. 4, pp. 407–14, 2004.

[16] —, "Prosthetic foot roll-over shapes with implications for alignment of trans-tibial prostheses," *Prosthet. Orthot. Int.*, vol. 24, no. 3, pp. 205–15, 2000.

[17] F. C. Anderson and M. G. Pandy, "Individual muscle contributions to support in normal walking," *Gait Posture*, vol. 17, no. 2, pp. 159–69, 2003.

[18] R. M. Murray, Z. Li, and S. S. Sastry, *A Mathematical Introduction to Robotic Manipulation*, 1st ed. Boca Raton, FL: CRC Press, 1994.

[19] A. Isidori, *Nonlinear Control Systems*, 3rd ed. Springer, 1995.

[20] K. Akbari Hamed, B. G. Buss, and J. W. Grizzle, "Continuous-time controllers for stabilizing periodic orbits of hybrid systems: Application to an underactuated 3D bipedal robot," in *IEEE 53rd Annu. Conf. Decision Control (CDC)*, 2014, pp. 1507–13.

[21] B. Morris and J. W. Grizzle, "A restricted poincaré map for determining exponentially stable periodic orbits in systems with impulse effects: Application to bipedal robots," in *IEEE Decis. Contr. P.*, 2005, pp. 4199–206.